

### Short Communication

## A nickel–iron battery with roll-compacted iron electrodes

M.K. Ravikumar, T.S. Balasubramanian<sup>1</sup>, A.K. Shukla<sup>\*</sup>

*Solid State and Structural Chemistry Unit, Indian Institute of Science, Bangalore-560012, India*

Received 2 June 1995; accepted 3 August 1995

#### Abstract

The performance of a 6 V/6 Ah, commercial size, nickel–iron battery with roll-compacted iron electrodes is reported in terms of its discharge characteristics and cycle-life data. The battery can withstand prolonged charge/discharge schedules with little deterioration in its performance. The effect of varying discharge rate and temperature on the performance of a 1.2 V/2.5 Ah nickel–iron cell is also examined.

*Keywords:* Electrodes; Iron; Nickel–iron batteries

#### 1. Introduction

Nickel–iron batteries are attractive systems by virtue of their long cycle life (typically 3000 cycles) even under adverse operational conditions such as overcharge, overdischarge, charge stand, discharge stand, and inadequate maintenance [1–5]. Various types of iron electrodes have been developed for these batteries, i.e., sintered, pocket and rolled types. The rolled-type iron electrodes are commercially the most feasible. This is because they are cheaper than sintered types and exhibit better performance than pocket types. The problems that adversely affect the performance of iron electrodes are: (i) spontaneous corrosion in the charged state, which leads to a high rate of self-discharge; (ii) low faradaic efficiency for the anodic dissolution of iron, which forces a low utilization coefficient [6–10]. Over a decade of effort, the authors have been able to circumvent these problems to a substantial degree [11–17].

In this communication, we report the performance of a commercial size, 1.2 V/2.5 Ah nickel–iron cell and a commercial size, 6 V/6 Ah nickel–iron battery both with a positive-limited configuration and roll-compacted iron electrodes that have been developed in house. The effect of varying discharge rate and operational temperature on the performance of the cell have been studied. Cycle-life tests performed both on the cell and the battery indicate that these can deliver their rated capacities over prolonged charge/discharge schedules.

#### 2. Commercial size, 1.2 V/2.5 Ah nickel–iron cell

##### 2.1. Preparation, fabrication and formation of roll-compacted, iron negative electrodes

The preparation of the active material for the iron electrodes has been described in Ref. [11]. In brief, the active material is obtained by vacuum decomposition of iron oxalate at 773 K. The resulting mixture of Fe and Fe<sub>3</sub>O<sub>4</sub> is suspended in 1 wt.% KOH solution in required amounts and mixed in an ultrasonic agitator with 10 wt.% powdered graphite, 1 wt.% Bi<sub>2</sub>S<sub>3</sub> and 0.5 wt.% NiSO<sub>4</sub>. To this slurry, 6 wt.% polytetrafluoroethylene (PTFE)-GP2 Fluon suspension is added, drop by drop. The resulting putty-like mass is rolled against a smooth steel plate. The rolled sheet of the active material with additives is folded around a degreased nickel mesh (dimensions: 50 mm × 65 mm × 1 mm) and pressed at the optimum compaction pressure of 675 kg cm<sup>-2</sup> for 5 min. The roll-compacted electrodes are heat-treated in a stream of nitrogen at 573 K for 30 min.

Iron electrodes, thus prepared, are subjected to formation in an electrochemical cell that contains 6 M KOH electrolyte with 1 wt.% LiOH. Sintered nickel oxide electrodes are placed on either side of the iron electrode. Usually, iron electrodes are formed with 3–5 charge/discharge cycles. During the first cycle, the electrodes are charged at the C/20 rate for 16 h and, subsequently, at the C/10 rate. The electrodes are typically discharged at the C/5 rate. The formed iron electrode are inserted into pockets made out of the separator cloth.

<sup>\*</sup> Corresponding author.

<sup>1</sup> Present address: Renewable Energy Systems Ltd., Hyderabad-500855, India.

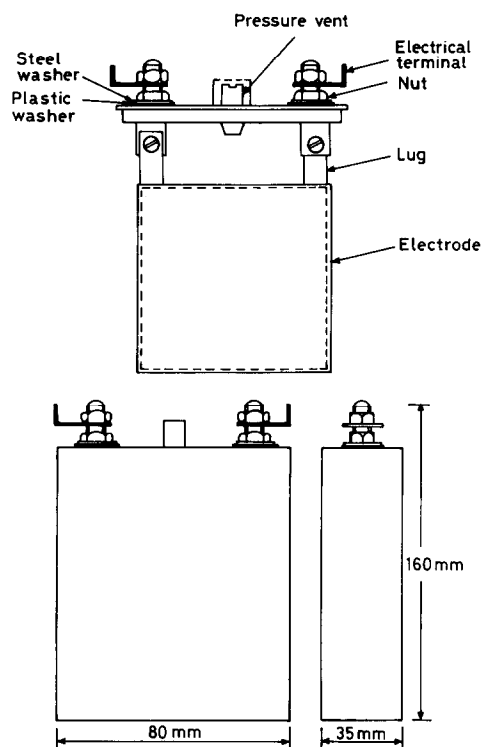


Fig. 1. Schematic setup of the nickel-iron cell.

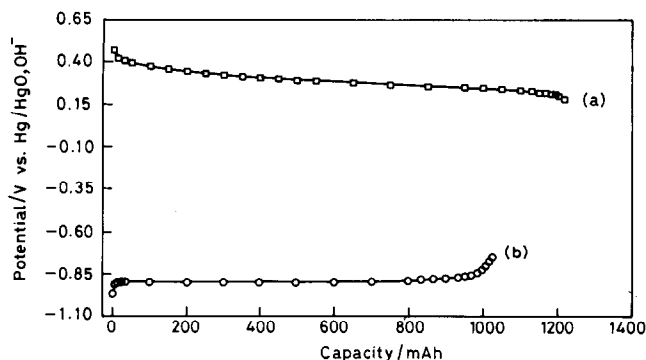


Fig. 2. Typical capacity data for individual: (a) nickel positive electrode (discharge current = 600 mA), and (b) iron negative electrode (discharge current = 200 mA).

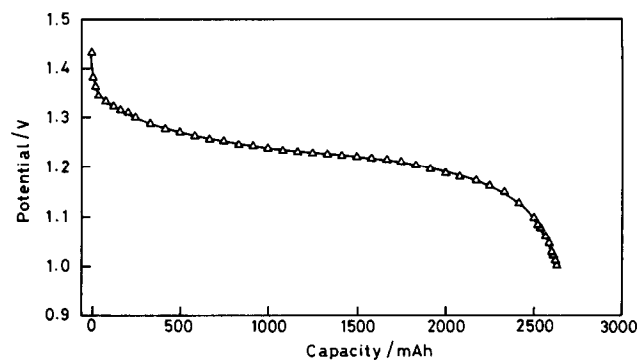


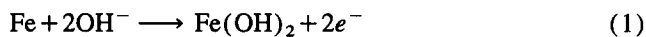
Fig. 3. Capacity data for nickel-iron cell at  $C/5$  discharge rate (corresponding current = 500 mA) to a cutoff voltage of 1 V.

## 2.2. Cell assembly

The positive-limited, nickel-iron secondary cell is assembled by alternatively stacking two commercial grade nickel positive electrodes (average capacity: 1.25 Ah) and three iron negative electrodes (average capacity: 0.95 Ah). The electrodes are connected with their respective lugs (as shown in Fig. 1) and then placed into polypropylene container (dimensions: 80 mm  $\times$  160 mm  $\times$  38 mm) that can withstand a concentrated alkali environment without deterioration over prolonged durations and at temperatures up to about 65 °C. The cell is filled with 6 M KOH electrolyte that contains 1 wt.% LiOH so as to immerse completely the electrodes.

## 2.3. Performance characteristics of nickel-iron cell

Typical data on the discharge characteristics of the roll-compacted iron negative and nickel positive electrodes employed in the assembly of the 1.2 V/2.5 Ah nickel-iron cell are shown in Fig. 2. The iron electrodes are discharged up to -860 mV versus a Hg/HgO, OH<sup>-</sup> reference electrode. This corresponds to the first discharge step of the iron electrode reaction, expressed as [2]:



On average, the electrodes delivered a capacity of  $\sim 0.95$  Ah ( $\sim 250$  mAh  $g^{-1}$ ) at the  $C/5$  rate (corresponding current: 200 mA)<sup>2</sup>. The nickel positive electrodes gave an average capacity of 1.25 Ah at the  $C/2$  rate. The capacity of the nickel positive electrodes exhibits little change at different rates between  $C$  and  $C/5$ .

Discharge data at the  $C/5$  rate for a positive-limited 1.2 V/2.5 Ah cell that comprises two nickel positives and three iron negatives are shown in Fig. 3. The cell displays an initial drop of 50 mV; this indicates that the internal resistance is  $\sim 100$  m $\Omega$ . The cell delivers a capacity of 2.5 Ah to a cutoff

<sup>2</sup> Roll-compacted iron electrodes prepared from active material obtained by vacuum decomposition of in situ prepared Bi<sub>2</sub>S<sub>3</sub> with ferrous oxalate precipitated on to graphite powder are found to deliver capacity values close to  $300 \pm 10$  mAh  $g^{-1}$  to a cutoff potential of -0.860 V. The Bi<sub>2</sub>S<sub>3</sub> is obtained with ferrous oxalate by the reaction of appropriate quantities of Bi(NO<sub>3</sub>)<sub>3</sub> and Na<sub>2</sub>S<sub>2</sub>O<sub>3</sub>.

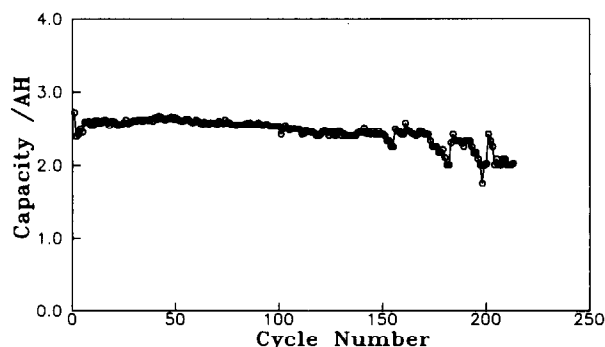


Fig. 4. Cycle-life data for nickel-iron cell.

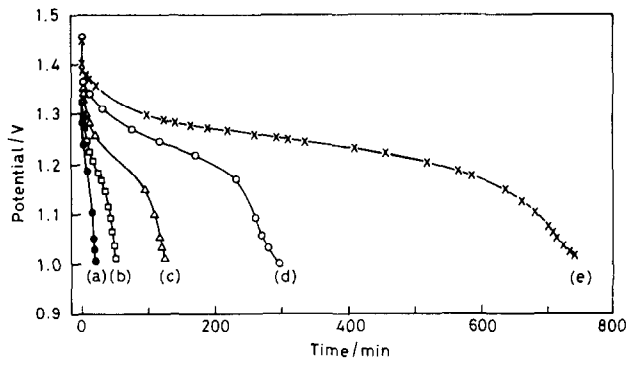


Fig. 5. Performance of nickel-iron cell at various discharge currents (mA): (a) 1800; (b) 1250; (c) 750; (d) 400, and (e) 200.

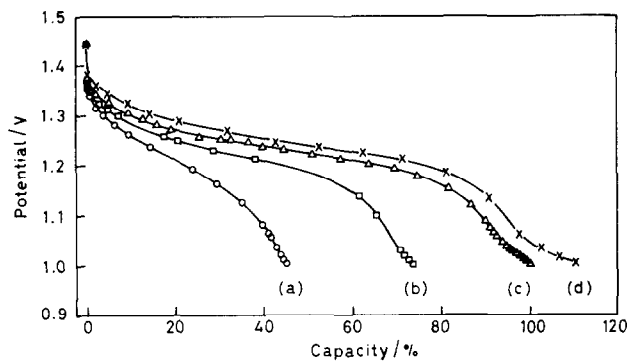


Fig. 6. Effect of temperature on capacity of nickel-iron cell at C/5 discharge rate. Temperature (°C): (a) 8; (b) 18; (c) 25, and (d) 35.

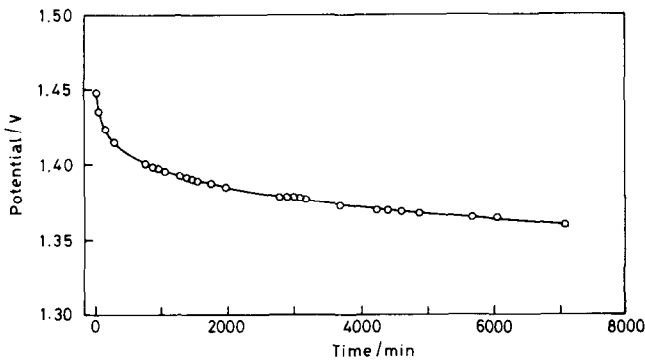


Fig. 7. Variation in open-circuit voltage of nickel-iron cell during 120 h charge stand.

voltage of 1 V. The cycle-life data are given in Fig. 4. To date, the cell has completed 200 charge/discharge cycles without any noticeable decay in its rated capacity. The performance of the cell at different discharge rates is presented in Fig. 5.

The effect of temperature on the discharge characteristics of the 1.2 V/2.5 Ah cell at the C/5 rate is shown in Fig. 6. The cell suffers a capacity loss of ~65% at 8 °C in comparison with its capacity at 25 °C. By contrast, there is a corresponding gain in capacity of ~10% at 35 °C. The reduced capacity at low temperatures could be due to: decreased solubility of the reaction intermediates; increased resistance and

viscosity of the electrolyte, and slower reaction kinetics at the electrodes [5].

The cell has been subjected to a charge stand for 120 h. The resulting change in open-circuit voltage is given in Fig. 7. The discharge data subsequent to the charge stand is presented in Fig. 8. The results show a loss of about 25% from the initial capacity. There is also a higher initial drop during cell discharge. This suggests a build-up in the internal resistance of the cell due to formation of Fe(OH)<sub>2</sub> at the iron electrodes and Ni(OH)<sub>2</sub> at the nickel electrodes. The nickel-iron cell has also been upgraded to 25 Ah unit. The discharge data at the C/5 rate are shown in Fig. 9.

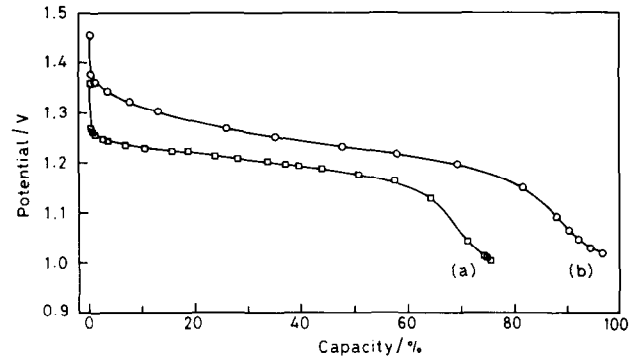


Fig. 8. Capacity retention data for nickel-iron cell: (a) after charge stand for 120 h, and (b) subsequent to immediate charge.

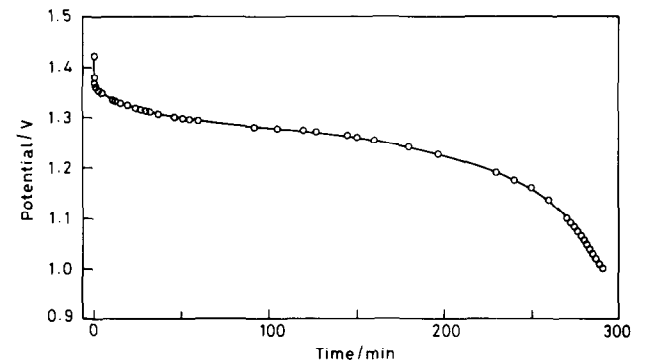


Fig. 9. Discharge data for 1.2 V/25 Ah nickel-iron cell at C/5 discharge rate (corresponding current = 5 A).

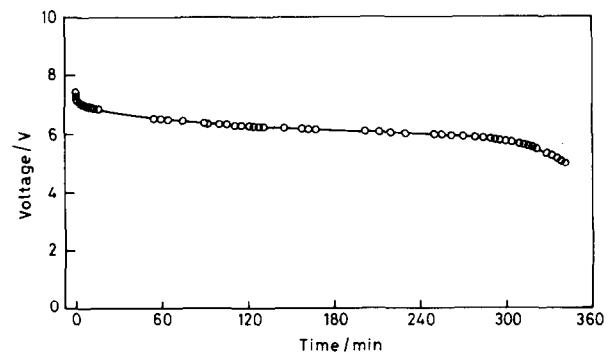


Fig. 10. Discharge data for 6 V/6 Ah nickel-iron battery at C/5 rate.

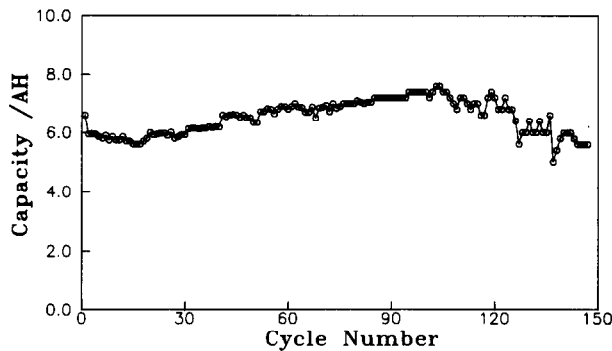


Fig. 11. Cycle-life data for 6 V/6 Ah nickel-iron battery.

### 3. Performance of 6 V/6 Ah nickel-iron battery

A commercial grade 6 V/6 Ah nickel-iron battery has been assembled by coupling five 1.2 V/6 Ah cells. The discharge data at the  $C/5$  rate are given in Fig. 10 and the cycle-life performance in Fig. 11. To date, the battery has completed about 150 cycles with little deterioration in rated capacity.

### References

- [1] A.K. Shukla, M.K. Ravikumar and T.S. Balasubramanian, *J. Power Sources*, 51 (1995) 29.
- [2] L. Öjefors, *Studies on the Alkaline Iron Electrodes*, Swedish National Development Co., Royal Institute of Technology, Stockholm, 1978.
- [3] M. Sittig, *Hazardous and Toxic Effects of Industrial Chemicals*, Noyes Data Corporation, NJ, USA, 1979.
- [4] S.U. Falk and A.J. Salkind, *Alkaline Storage Batteries*, Wiley, New York, 1964.
- [5] D. Linden, *Handbook of Batteries and Fuel Cells*, McGraw-Hill, New York, 1984.
- [6] L. Öjefors, *Electrochim. Acta*, 21 (1976) 263.
- [7] P. Hersh, *Trans. Faraday Soc.*, 51 (1955) 1442.
- [8] V.J. Linnerbom, *J. Electrochem. Soc.*, 105 (1958) 322.
- [9] S. Hills, *J. Electrochem. Soc.*, 112 (1966) 1048.
- [10] T.S. Lee, *J. Electrochem. Soc.*, 118 (1971) 1278.
- [11] K. Vijayamohan, A.K. Shukla and S. Sathyanarayana, *Indian J. Technol.*, 24 (1986) 430.
- [12] K. Vijayamohan, A.K. Shukla and S. Sathyanarayana, *J. Power Sources*, 32 (1990) 339.
- [13] K. Vijayamohan, A.K. Shukla and S. Sathyanarayana, *J. Electroanal. Chem.*, 289 (1990) 55.
- [14] K. Vijayamohan, A.K. Shukla and S. Sathyanarayana, *Electrochim. Acta*, 36 (1990) 369.
- [15] K. Vijayamohan, A.K. Shukla and S. Sathyanarayana, *J. Electroanal. Chem.*, 295 (1990) 59.
- [16] T.S. Balasubramanian and A.K. Shukla, *J. Power Sources*, 41 (1993) 99.
- [17] T.S. Balasubramanian, K. Vijayamohan and A.K. Shukla, *J. Appl. Electrochem.*, 23 (1993) 947.